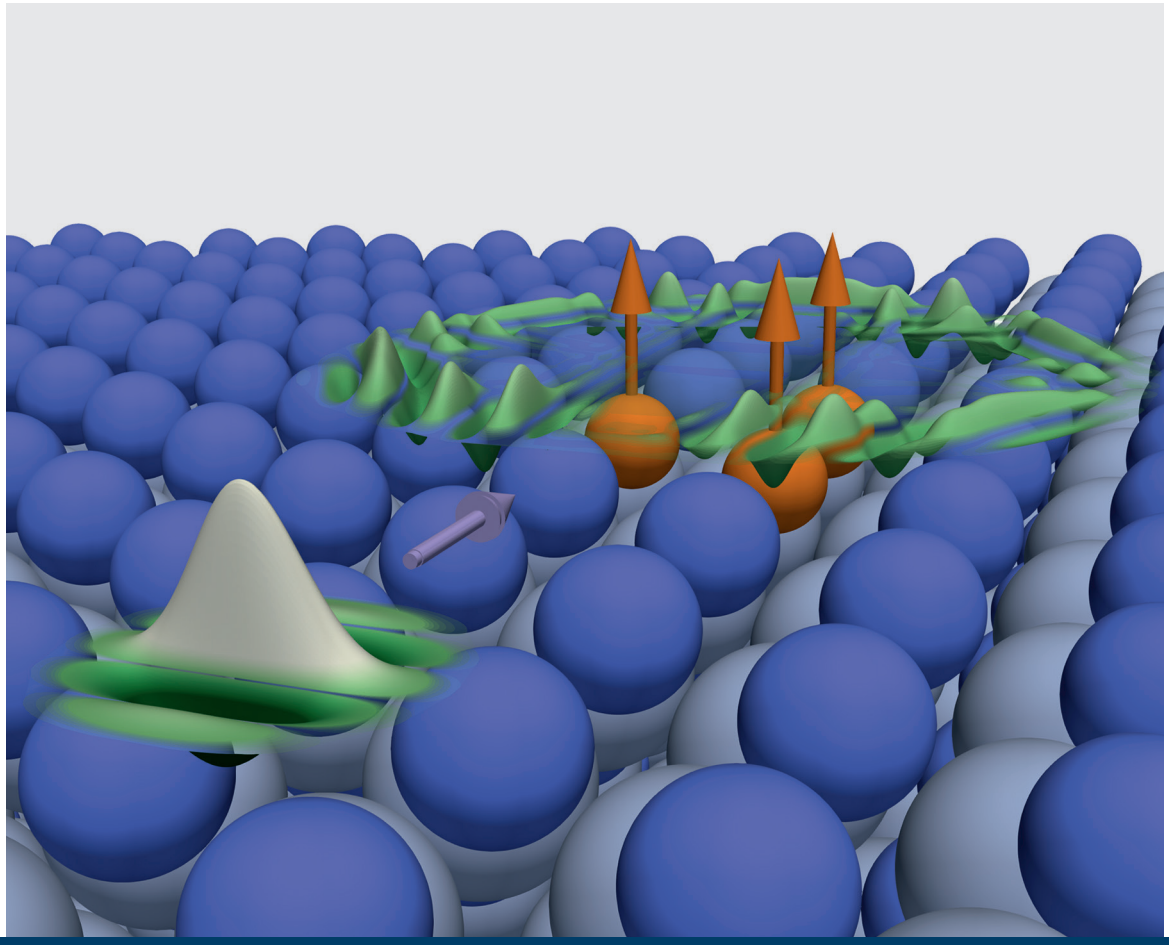

Spin scattering of topologically protected electrons at defects

Philipp Rüßmann

Schlüsseltechnologien / Key Technologies
Band / Volume 173
ISBN 978-3-95806-336-5

Mitglied der Helmholtz-Gemeinschaft

JÜLICH
Forschungszentrum

Forschungszentrum Jülich GmbH
Peter Grünberg Institut (PGI)
Quanten-Theorie der Materialien (PGI-1/IAS-1)

Spin scattering of topologically protected electrons at defects

Philipp Rüßmann

Schriften des Forschungszentrums Jülich
Reihe Schlüsseltechnologien / Key Technologies Band / Volume 173

ISSN 1866-1807 ISBN 978-3-95806-336-5

Contents

1. Introduction **1**

2. Basic theory **7**
2.1. A short introduction to density functional theory 7
2.2. The Korringa-Kohn-Rostoker Green function method 9
2.2.1. Green functions in solid state physics 10
2.2.2. Ab-initio computation of the Green function within the KKR-GF formalism 11
2.2.3. Beyond the crystalline solid: Impurity embedding and elastic scattering off impurities 13
2.2.4. Summary of the KKR-GF method 16
2.3. Introduction to topology in solid state physics at the example topological insulators 16
2.3.1. Topology in band structures 16
2.3.2. Connection between topology and physical observables 17
2.3.3. Bulk-boundary correspondence and topological protection 19
2.3.4. Other topologically nontrivial solids apart from topological insulators 21

3. Parallelization of the *KKRcode* **23**
3.1. Introduction 23
3.1.1. The state of the art in HPC architecture and parallel programming models 26
3.1.2. Parallel performance and scaling laws 28
3.2. Implementation of hybrid parallelism in KKR 30
3.2.1. Parallelization scheme - levels 1 and 2: parallelization with MPI . . . 30
3.2.2. Parallelization scheme - level 3: parallelization with OpenMP 34
3.3. Performance of the two-level MPI parallel implementation in the *KKRcode* . 36
3.3.1. Trace analysis of level 1 - MPI: parallelization over energies 37
3.3.2. Trace analysis of level 2 - MPI: parallelization over atoms 40
3.3.3. The load imbalance problem 42
3.4. Strong and weak scaling behavior of the hybrid MPI/OpenMP parallelization 45
3.4.1. Parallel performance of the two level MPI: strong and weak scaling . 45
3.4.2. The scaling behavior of the OpenMP level in the hybrid implementation 48
3.5. Conclusions and outlook 50

4. Revealing scattering properties of topologically protected electrons 51
4.1. Introduction . . . 52
4.2. Electron scattering off defects and standing waves around impurities on TIs . 54
4.2.1. Scattering of topologically protected surface state electrons off defects at the surface of Bi_2Te_3 . . . 54
4.2.2. Ab-initio calculation of scattering probabilities for non-magnetic defects 57
4.2.3. Ab-initio calculation of scattering probabilities for magnetic defects . 61
4.2.4. Seeing scattering processes in real-space: QPI images . . . 67
4.3. Green function and $\mathcal{T}$-matrix approach to the quasiparticle interference on surfaces . . . 71
4.3.1. The general formalism . . . 71
4.3.2. Model calculations for the QPI on Bi_2Te_3 . . . 76
4.3.3. An *ad-hoc* approach: The joint density of states and beyond . . . 79
4.4. QPI calculations within the KKR formalism: the "real thing" . . . 89
4.4.1. Theoretical description of the QPI in reciprocal space within the language of the KKR method . . . 89
4.4.2. Results of QPI calculations for different defects in Bi_2Te_3 within the ab-initio KKR formalism . . . 91
4.5. Conclusion and outlook . . . 94

5. Superparamagnetism-induced mesoscopic electron focusing in topological insulators 97
5.1. Introduction . . . 98
5.2. Seeing electron focusing and backscattering in real and reciprocal space via STM . . . 99
5.3. Explanation of the observations: calculations and discussion . . . 103
5.3.1. Details of the calculations . . . 103
5.3.2. On the importance of magnetic order: uniform background magnetization 105
5.3.3. Tailoring the backscattering amplitude: strong magnetic scattering centers . . . 107
5.4. Experimental signatures of magnetism in Mn-doped Bi_2Te_3 via XMCD . . . 110
5.5. Conclusions and outlook . . . 112

6. Lifetime and surface-to-bulk scattering of the TSS in 3D TIs 113
6.1. Introduction . . . 114
6.2. Energy dependent lifetime and scattering rates of the topological surface state in Bi_2Te_3 . . . 115
6.2.1. Numerical details of the calculation . . . 115
6.2.2. Anisotropic lifetime of the surface state in Bi_2Te_3 . . . 117
6.2.3. Resonant scattering of the topological surface state in Bi_2Te_3 . . . 119
6.2.4. On the importance of the scattering phase space end-states: understanding the surface-to-bulk scattering rates . . . 120
6.3. The influence of the warping strength: comparison to Bi_2Se_3 . . . 121
6.4. Conclusion and outlook . . . 123

7. Exchange interactions on magnetically doped topological Insulators 125
7.1. Introduction . . . 126
7.1.1. Competing mechanisms of the exchange interaction . . . 127
7.2. Experimental observation of magnetism in surface-doped Bi_2Te_3 . . . 131
7.2.1. Experimental setup . . . 133
7.2.2. Experimental results . . . 133
7.3. Microscopic origin of the exchange mechanism in Bi_2Te_3 and comparison to experiment . . . 135
7.3.1. Setup of calculation and computation details . . . 135
7.3.2. Spatially anisotropic exchange coupling in transition metal doped Bi_2Te_3 139
7.3.3. Competing exchange mechanisms in Mn, Fe and Co surface-doped Bi_2Te_3 . . . 142
7.3.4. Comparison to experiment . . . 150
7.3.5. Tailoring the exchange interaction: doping dependence . . . 153
7.3.6. The high concentration limit: nearest-neighbor dimer and trimer . . . 160
7.4. Conclusions and outlook . . . 165

8. Universal response to impurities in the type-II Weyl semimetal phase diagram 167
8.1. Introduction . . . 168
8.2. $Mo_xW_{1-x}Te_2$: a type-II Weyl semimetal? . . . 170
8.2.1. Computational details . . . 173
8.2.2. Ab-initio surface band structures of WTe_2 and $MoTe_2$ in comparison to ARPES measurements . . . 178
8.3. QPI signature of the scattering properties of Fermi arcs in WTe_2 and $MoTe_2$ 179
8.3.1. Quasiparticle interference on the surface of type-II Weyl semimetal candidates WTe_2 and $MoTe_2$ . . . 181
8.3.2. Energy dependence of Fermi arc scattering in $MoTe_2$ . . . 182
8.4. Impurity resonances in $MoTe_2$ and WTe_2 . . . 185
8.5. Conclusions and outlook . . . 187

9. Conclusions and outlook 189

A. Appendix 193
A.1. Implementation details of the FT-QPI calculation within KKR . . . 193
A.1.1. Construction of $\mathcal{G}^{\text{host}}$ . . . 193
A.1.2. Impurity scattering path operator . . . 194
A.1.3. Calculation of the prefactor . . . 194
A.2. Used Software packages . . . 195

Bibliography 197

Schlüsseltechnologien / Key Technologies
Band / Volume 173
ISBN 978-3-95806-336-5

Mitglied der Helmholtz-Gemeinschaft

JÜLICH
Forschungszentrum